A Wide-Angle Scanning Planar Phased Array with Pattern Reconfigurable Magnetic Current Element

A Wide-Angle Scanning Planar Phased Array with Pattern Reconfigurable Magnetic Current Element

Xiao Ding, You-Feng Cheng, Wei Shao, Hua Li,
Bing-Zhong Wang, and Dimitris E. Anagnostou

***Abstract*— A wide-angle scanning planar phased array with magnetic current elements is proposed. A pattern reconfigurable technique is used to design the element that enhances scanning gain and decreases the sidelobe level throughout the entire scanning range. The array is comprised of eight elements in a 2×4 arrangement with uniform spacing. The proposed phased array operates at 5.8 GHz and can scan with 3 dB beamwidth the entire upper ground elevation plane from -90° to $+90^\circ$ enabled by a two-step pattern reconfigurability mechanism consisting of: 1) coarse-angle scanning and 2) fine-angle scanning. Significant outcomes also include the reduced sidelobe level (less than 7.8 dB) and the particularly small fluctuation (± 0.75 dB) of the gain during scanning over a scanning range of 150° (from -75° to $+75^\circ$ in the elevation plane). With the absence of any structure above the ground level, the high efficiency, and the coverage of the entire upper half-space, this proposed antenna array is very attractive for a variety of phased array applications, particularly those that require a flush-mounted structure.**

***Index Terms*— Antenna arrays, pattern reconfigurable antennas, planar phased arrays, wide-angle beam scanning.**

I. Introduction

Planar phased arrays often require a large ground plane. Specifically, the large ground plane can be considered as an electric or magnetic wall [1]. The analysis conducted in [2] and [3] showed that an electric wall phased array can only scan its main beam direction from -50° to 50° with a gain fluctuation of 4–5 dB, because the beamwidths of the elements in an electric wall phased array are limited, and mutual coupling between elements is strong when the beam is scanned at low elevation (near endfire) angles [4]–[6]. Many related efforts have been carried out to break the bottleneck of the limitation scanning angles. It include a multipanel approach method [7], a wide-beam element method [8], a metasurface technique [9], pattern reconfiguration technique [10]–[12], a mutual coupling reduction method [13], and others.

Among these methods, pattern reconfigurable techniques have been popular and have seen a wide range of applications. For example, a pattern reconfigurable array can collect energy from several switchable directions, and can enhance channel capacity in massive-MIMO communication systems by using pattern diversity.

In this communication, the main challenge and novelty consist of the development and use of flush-mounted slot antenna elements and pattern reconfigurable techniques for the design and creation of a phased array with outstanding wide-angle scanning performance. Specifically, the antenna elements can reconfigure narrow beams to jointly cover the entire top half-space, and thus enable wide-angle scanning. Compared to prior art, it will be shown how slot elements with electric wall modeling are used to reconfigure the pattern and how the scanning performance will be improved (meaning lower sidelobe level, small fluctuation of the gain during scanning, high efficiency, and entire plane of the upper half-space beam coverage). This communication complements well prior research on fundamental wide-angle scanning arrays.

In addition, pattern reconfigurable techniques used in wide-angle scanning arrays have been described. In [10], a millimeter-wave pattern reconfigurable 1×4 linear wide angle scanning phased subarray with reconfigurable feeding networks was design. By dividing the scanning space into multiple regions, a Yagi microstrip antenna using reconfigurable radiating elements comprised a nonuniform linear phased array that could scan up to a maximum of approximately $\pm 60^\circ$ with low sidelobe level [12]. In this communication, the proposed phased array can scan with 3 dB beamwidth that covers an entire plane of the upper elevation plane from -90° to $+90^\circ$, representing a scan covering area improvement of 33% over microstrip elements. First, a novel pattern reconfigurable magnetic current element and its principle of operation are introduced. Then, a 2×4 wide-angle scanning carrier-based planar phased array is proposed and developed. Finally, the wide-angle scanning performance of the proposed phased array is analyzed.

II. Pattern Reconfigurable Magnetic Current Element

A. Element Design

The simplest model of a magnetic current radiator is an aperture antenna, which has an equivalent magnetic current distribution inside the slot parallel to the ground plane. In this situation, the sum of the maximum electric field generated by the magnetic current source and its image source will occur in the endfire direction [14], and the electric field can potentially cover that direction of radiation. This arrangement benefits by achieving wide-angle scanning performance.

The proposed reconfigurable element is based on the boxed-in slot antenna [15], which is cavity-backed and then converted to a Yagi slot [16] by using additional slots as directors or reflector. The structure of the proposed element can be seen as the complementary structure of the printed Yagi antenna [17]. The cavity helps maintain a unidirectional pattern. By altering the length of the slots using p-i-n diodes, the electromagnetic wave can be guided or reflected to or from a specific direction. The geometry of this basic reconfigurable element is shown in Fig. 1.

The basic element comprises five apertures that are carved on a metal ground $L_0 \times W_0$. The center slot $L_S \times W_S$ is excited by using the tip of a coaxial cable that is soldered off-center at the feeding positon L_f for impedance matching purposes, as shown in Fig. 1(b). The additional four slots are parasitic. Their dimensions are $L_1 \times W_1$, and they act as the aforementioned director or reflector depending on how they are configured. In this way, the top layer of the Yagi slot antenna is formed.

Next, a hollow metallic box cavity $L_b \times W_b$ with height $H_b = \lambda/4$ is placed just underneath the excitation slot as shown in Fig. 2(c) and (d) to form the necessary unidirectional pattern and enhance directivity. Under the metal ground, a microstrip substrate ($H_0 = 1$ mm, $\varepsilon_r = 2.2$) is placed and on the backside of the substrate four metallic strips are printed between the above-mentioned slots. In this way, the bottom layer of the Yagi slot antenna is formed.

Third, eight p-i-n diode switches (S_1 through S_8) [18] are grouped in pairs and are embedded in the eight gaps on the strip layer,

Manuscript received June 9, 2016; revised November 4, 2016; accepted November 25, 2016. This work was supported in part by the National Natural Science Foundation of China under Grant #61331007, Grant #61361166008, and Grant #61401065, in part by the U.S. National Science Foundation under Grant #1310400, and in part by the National Aeronautics and Space Administration, EPSCoR, under Grant #NNX15AM83A.

X. Ding, Y.-F. Cheng, W. Shao, H. Li, and B.-Z. Wang are with the Institute of Applied Physics, University of Electronic Science and Technology of China, Chengdu 610054, China (e-mail: xding@uestc.edu.cn; juvencheng1377@gmail.com; weishao@uestc.edu.cn; lihua2006@uestc.edu.cn; bzwang@uestc.edu.cn).

D. E. Anagnostou is with Heriot-Watt University, Edinburgh EH14 4AS, U.K., and also with the South Dakota School of Mines and Technology, Rapid City, SD 57701 USA (e-mail: danagn@ieee.org).

Color versions of one or more of the figures in this communication are available online at http://ieeexplore.ieee.org.

Digital Object Identifier 10.1109/TAP.2016.2637863

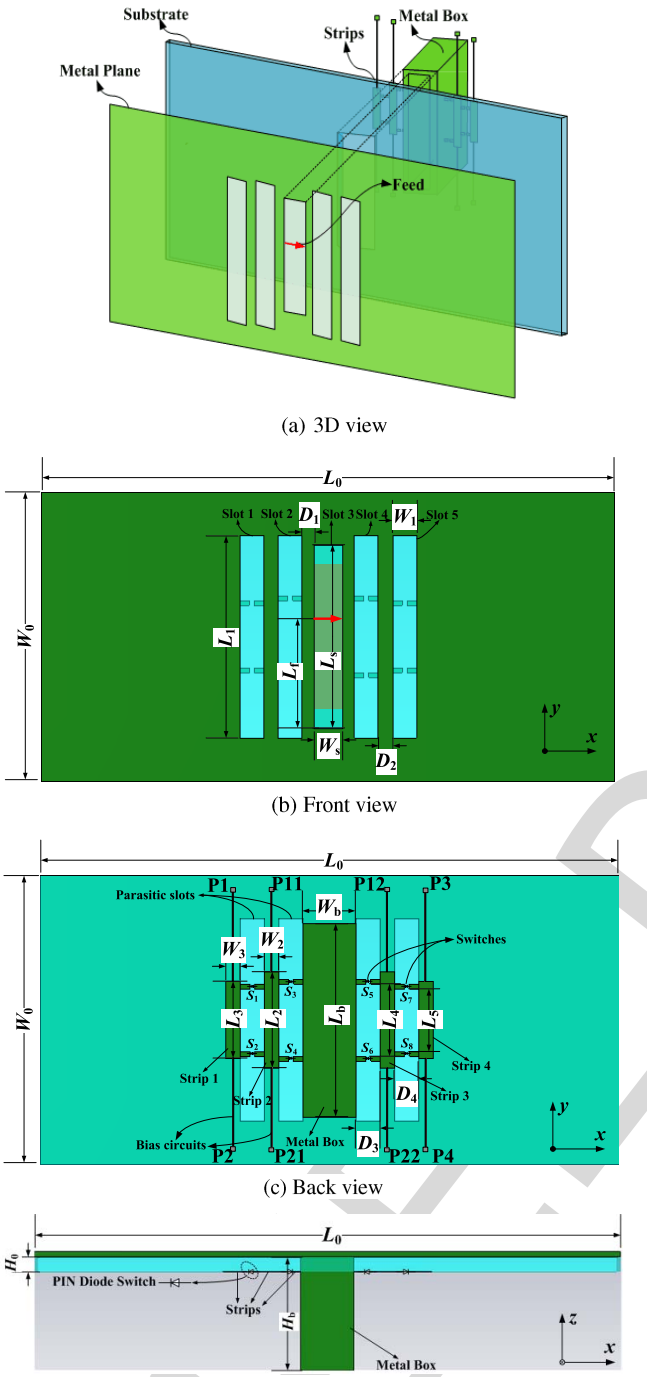

Fig. 1. Structure of the proposed pattern reconfigurable element. (a) 3-D view, (b) front view, (c) detailed back view including the p-i-n diodes, dc bias-circuits, and dc/grounded connection nodes, and (d) side view, showing the structure, the diode placement, and polarity.

as shown in Fig. 1(c). The diodes allow adjusting the electrical length of the parasitic slots by applying a dc biasing voltage, without needing a bandwidth-limiting biasing network [19], [20]. In this way, the slots can act as directors or reflectors on-demand, allowing steering the beam in specific directions. To bias the diodes, a dc voltage is applied to the p-i-n diodes through metal pads at points P12 to P22, while nodes P1–P4 are connected to the ground.

Finally, The operating frequency is determined by the dimensions of the excitation slot and is set here at 5.8 GHz. Adjustment of the

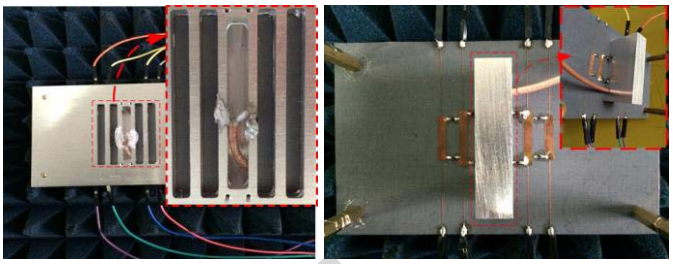

Fig. 2. Photographs of the reconfigurable element. (a) Top view including feeding position and white plastic adhesive. (b) Back view including coaxial feeding cable, hollow metallic box with a hole in the side, dc bias-circuits, and p-i-n diodes.

TABLE I
PHYSICAL ANTENNA DIMENSIONS

Parameter	Value (mm)	Parameter	Value (mm)	Parameter	Value (mm)
L_0	120	L_2, L_4	20	W_1	5
L_S	38	L_3, L_5	16	W_2, W_3	3
L_b	40	W_0	70	D_1	2.5
L_f	32.5	W_S	6	D_2	3
L_1	42	W_b	11	D_3, D_4	5

size and position of the coplanar parasitic slots and of the noncoplanar strips is necessary as they relate to the excitation slot according to the operating principle of the Yagi antenna.

Fig. 2 shows the photo of the proposed reconfigurable element, and the inset images show details of the expanded connection part of the center. It is noteworthy that a small hole is opened on one side of the hollow metallic box, for the feeding coaxial cable to pass through and reach the top of the slot. The outer conductor of the cable is soldered to one side of the slot, and plastic adhesive is used to fix the bonding pad. The inner conductor of the cable is soldered to the other side of the slot and is also fixed with plastic adhesive. The physical parameters of the structure are summarized in Table I.

B. Reconfiguration Principle

The proposed basic antenna element can reconfigure its radiation pattern in three different directions, or modes. These are two tilted modes with higher directivity, and one broadside radiation mode at x-axis.

First, the first mode is enabled when P12 (or P22) is connected to the $V_{\text{bias}} = 3$ V, and P3 (or P4) is connected to ground [Fig. 1(c)]. When the diode switches S_5 through S_8 are ON, the strips at the right side connect together and the current distribution on that side is altered in a way that makes the RF current to pass through the p-i-n diodes and feed the right sided slots. This causes the electrical length of the right slots to become shorter than the left ones. The (smaller) right slots guide the electromagnetic radiation while the (larger) left slots reflect it. This steers the radiation pattern to the right. A detailed 3-D current distribution in this case is shown in Fig. 3.

Based on geometric structure and intuition, the effective length has been used to explain the reconfigurable patterns as above. A more detailed explanation is provided below. When all the diode switches in the left slot are OFF and more capacitance and inductance are introduced, then the resonant frequency of the parasitic slot decreases to be lower than that of the driven slot. When the antenna operates near the resonant frequency of the driven slot, the parasitic slot is inductive and acts as a reflector. At the same time, all the diode

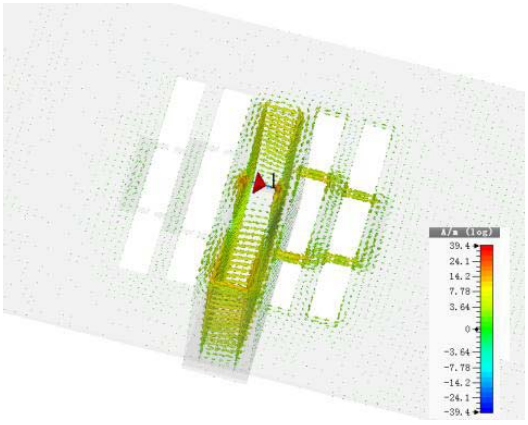

Fig. 3. 3-D current distribution of the reconfigurable element when the p-i-n diodes on the right side are activated, making the slots narrower. The right side slots direct the electromagnetic wave, while the larger slots on the left side reflect it.

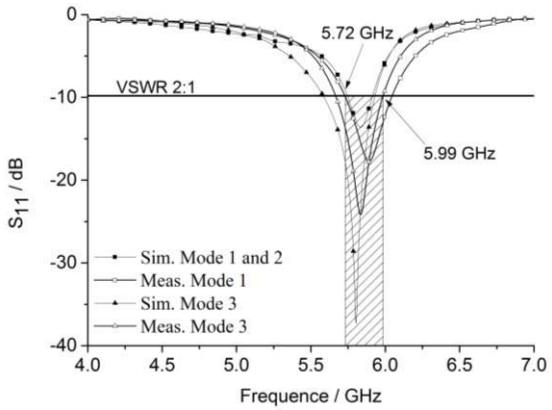

Fig. 4. Measured and simulated reflection coefficient of the antenna illustrating the similar bandwidth and matching for all configurations. Modes 1 and 2 are symmetric so only one is shown.

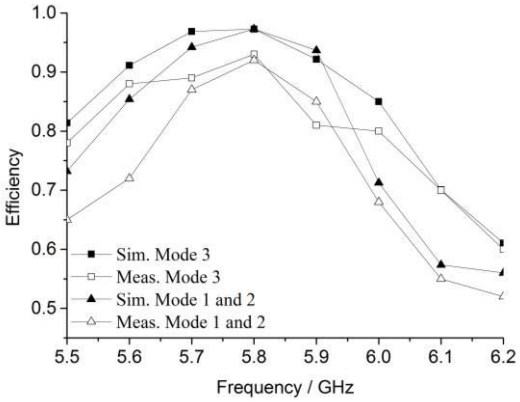

Fig. 5. Measured and simulated efficiencies of the antenna are very high (above 90%) at the resonant frequency.

switches in the right slot are ON, then the resonant frequency of the parasitic slot increases to be higher than that of the driven slot, the parasitic slot is capacitive and acts as a director at approximately the resonant frequency of the driven element.

Second, the second tilted mode can be obtained in the reverse way, by connecting P11 (or P21) to the V_{bias} and P1 (or P2) to the ground. This steers the radiation pattern to the left.

Finally, the third mode is obtained when all the diodes are OFF. Then, the excited slots radiates omnidirectionally like a traditional single slot antenna, at right angles to the largest dimension of the slot, while the box structure ensures a broadside direction with small front-to-back ratio.

Moreover, the control mechanism for the p-i-n diodes can be explained as follows. When P11 and P21 are connected to the power supply with $V_{\text{bias}} = 3$ V, S_1–S_4 are ON. When P12 and P22 are connected to the power supply with $V_{\text{bias}} = 3$ V, S_5–S_8 are ON. Since the bias lines are very narrow, the RF impedance is very high and little RF energy can get through it. Furthermore, the bias current has minimal impact on the antenna performance since the bias circuits are located below the ground plane and separated by the radiation slot.

C. Results and Analysis

The measured reflection coefficient at each mode is shown in Fig. 4. All modes have approximately the same bandwidth (5.7–6 GHz), as expected since the radiating element does not alter from configuration to configuration. The simulated and measured efficiencies of the antenna are very high as expected by the radiating element that is a metallic slot (Fig. 5).

Fig. 6 shows the radiating performance of the proposed antenna. The cross polarization patterns at each reconfigurable mode are below −20 dB. Also, due to the symmetry of the proposed structure, the radiation performance of Modes 1 and 2 [Fig. 6(a) and (b)] is almost symmetric. Moreover, the measured gain of Modes 1 and 2 is higher than 7 dBi. The pattern of Mode 3 [Fig. 6(c)] is indeed broadside about 5 dBi gain. The higher directivity of the tilted beam modes is conducive to the wide-angle scanning while the antenna maintains a high scanning gain level at large scanning angles.

The effect of varying the strips length [see Fig. 1(c)] on the copolarization and cross-polarization patterns of the proposed element was studied through Mode 2 as an example. Fig. 7 (below) was added to show the effect of the strips with varying length on the copolarization and cross-polarization patterns.

In Fig. 7, as the length of the strips increasing, the directivity of the element decreases gradually, the maximum radiation will point toward a lower elevation angle at −65° with increasing SLLs. On the other hand, decreasing the strips length steers the direction of maximum radiation to point toward a higher elevation angle at −55°, which means the element will not be able to cover the low elevation areas within its 3 dB beamwidth. In other word, compared to the 3 dB beamwidth obtained by the selected values, this joint 3 dB beamwidth become narrower. This narrow beamwidth is not good for wide-angle scanning.

In addition, a similar study was carried out to help understand how the length of the strips affects matching. Fig. 8 shows the S_{11} variation tendency when the length of the strips is varied. Increasing the length lowers the resonant frequency of the antenna. Decreasing the length increases the operation frequency while it degrades the matching. Since the strips are not on the driven element itself [Fig. 1(c)], they affect the driven element only through mutual coupling. Antenna matching is not affected as fields are not reflected back to the driven element to alter the excitation currents. This was accomplished through accurate selection of lengths of the D/R slots in a similar way to Yagi antennas.

III. Wide-Angle Scanning Phased Array and Its Scanning Performance

The aforementioned pattern reconfigurable antenna was next used to develop a 2×4 uniform wide-angle scanning planar phased array.

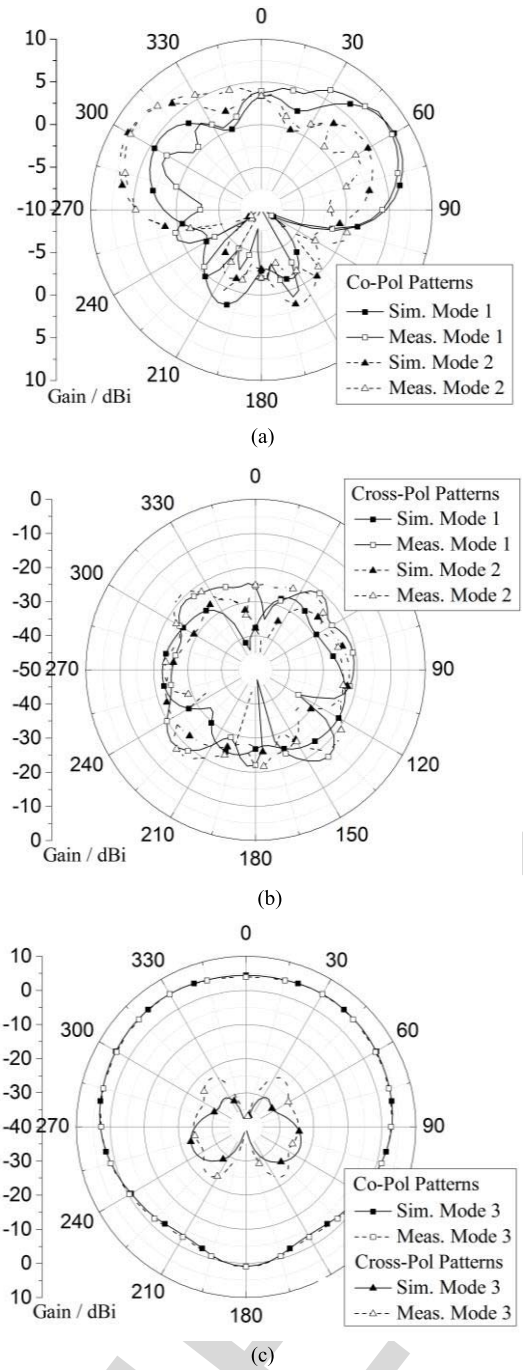

Fig. 6. Measured and simulated radiation patterns. (a) Copolarization of Mode 1 when the beam is steered to the right and Mode 2 when the beam is steered to the left. (b) Cross-polarization of Modes 1 and 2. (c) Third mode when the beam is not steered (broadside mode with flat gain). The measurements validate the simulations.

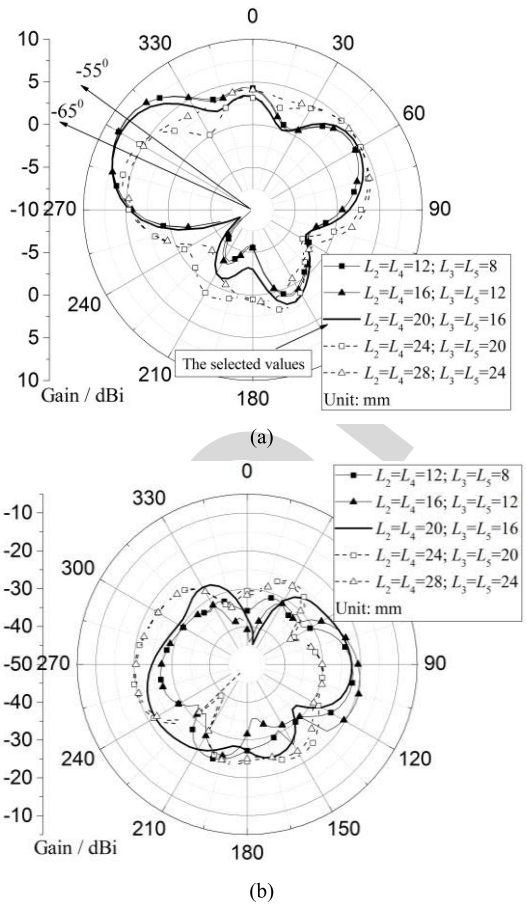

Fig. 7. Simulated radiation patterns at the second reconfigurable mode with variable strips length. (a) Copolarization patterns including the variation gain, direction of the maximum radiation, SLLs, and 3 dB beamwidth. (b) Cross-polarization always below −20 dB patterns.

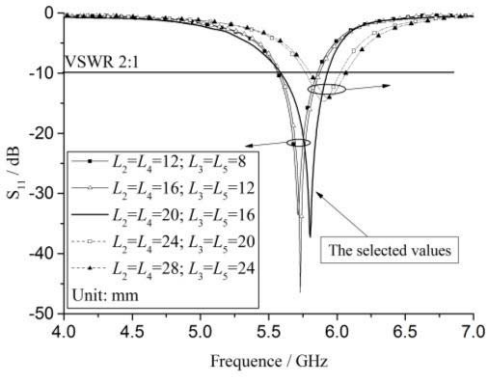

Fig. 8. Simulated S_{11} trends over variable strips length. Increasing the length lowers the resonant frequency of the antenna. Decreasing the length increases the operation frequency while it degrades the matching.

Next, a wide-angle scanning method with pattern reconfigurable techniques is presented first, and the scanning performance is analyzed.

A. Wide-Angle Scanning Array

A uniform wide-angle scanning carrier-based planar phased planar array was developed by combining eight of the proposed antennas in a 2×4 arrangement, and is shown in Fig. 9. The numbers ①, ②, … ⑧ represent each antenna's feeding port. It is worth noting that the structure of some elements on the array differs slightly from the proposed antenna. In order to reduce the spacing between adjacent elements, the two outer slots of the middle elements have been removed and the edge elements maintained their outer slots.

The distance between each element in the x-direction is set to $d_{\text{array}} = 0.54\lambda$, where λ is the free-space wavelength at 5.8 GHz and 0.6λ in y-direction. The total size of the phased array is 198 mm × 114 mm.

The designed 2×4 array was fabricated and is shown in Fig. 10, along with the measurement system that had to be developed and

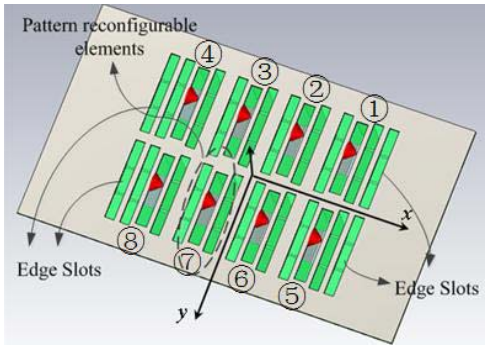

Fig. 9. Geometry of the wide-angle scanning phased array in a 2 × 4 arrangement.

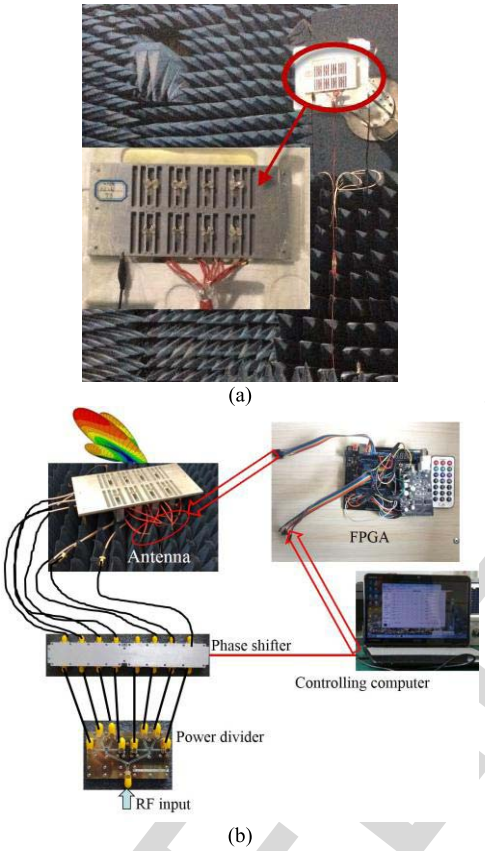

(a)

(b)

Fig. 10. (a) Photograph of the eight-element phased array measured in the anechoic chamber. (b) Photographs of the measurement system setup of the array.

which contains 6-b digital phase shifters, a 1:8 power divider, phase-compensated low-loss coaxial cables, an field-programmable gate array (FPGA) control device, and a control computer. In this setup, an FPGA provides a dc voltage to turn the p-i-n diodes ON or OFF, and control the operating reconfigurable modes. A 1:8 equal power divider is used to divide the input signal into eighths (i.e., the output signals at the output ports of the divider has equal amplitude and phase). Then the eight signals are supplied to eight phase shifters, where different phase differences are provided to the adjacent elements of the proposed array. During this process, the proposed phased array begins scanning.

The technique to realize wide-angle scanning in conjunction with pattern reconfigurability of the array is divided in two steps.

TABLE II

PERFORMANCE OF THE 2 × 4 PHASED ARRAY WITH PATTERN RECONFIGURABLE ELEMENTS

	Scanning performance values				3 dB joint cover range
	θ_{max}	Gain (dBi)	MSLL (dB)	Θ_{BW} 3dB	
Mode 1 (right steering)	+10°	15.5	-11.8	26°	-7° to +90°
	+25°	14.7	-9.3	32°	
	+35°	14.6	-10.8	31°	
	+55°	14	-8.5	37°	
	+65°	14.5	-8	38°	
	+75°	14.2	-7.8	37°	
	θ_{max}	Gain (dBi)	MSLL (dB)	Θ_{BW} 3dB	
Mode 2 (left steering)	-10°	15.5	-11.8	26°	-90° to +7°
	-25°	14.7	-9.4	32°	
	-35°	14.5	-10.8	31°	
	-55°	14.2	-8.6	36°	
	-65°	14.5	-8	38°	
	-75°	14.2	-7.7	36°	

1) *Coarse-Angle Scanning:* The scanning space of the array is divided into several subspaces and each subspace, respectively, matches with one of the reconfigurable narrow beams (modes) of the elements.
2) *Fine-Angle Scanning:* When all the reconfigurable elements have been set to a reconfigurable mode, beam scanning in the corresponding subspace can be fine-tuned by adjusting the phase shift of each element, as in traditional phased arrays.

B. Wide-Angle Scanning Performance

As mentioned earlier, the scanning space of this array is divided into two subspaces. Modes 1 and 2 are used to match these subspaces. When all elements are set to Mode 1, their scanning subspace (subspace 1) is from +10° to +75° in the *xoz* plane and the phase shifts between elements are provided by the 6-b phase shifters. In addition, when all elements are set to Mode 2, the scanning results can be obtained in subspace 2 (i.e., in the *xoz* plane from −75° to −10°).

The scanning performance was tested at 5.8 GHz with linear progressive phase shift from element to element. The array can scan subspaces 1 and 2 by pointing the main-lobe from $\theta = -75°$ to $+75°$ with extremely small fluctuation (±0.75°) of the gain during scanning over a scanning range of 150° (from −75° to +75°), while the 3 dB scanning beamwidth can cover a large range from −90° to +90° in the elevation plane. These are also shown by the scanning patterns in Fig. 11. The maximum scanning gain is 15.5 dBi and the minimum is 14 dBi, indicating less than 1.5 dB scanning gain fluctuation. This scanning performance is excellent for many applications in modern communication systems. The scanning gain, maximum peak sidelobe level (MSLL), scanning 3 dB beamwidth (BW), and the subspace range values are all listed in Table II.

A comparison between the proposed phased array and those in [10] and [12] are shown in Table III. The wide-angle scanning performance, including the peak-gain scanning range, 3-dB beamwidth coverage, peak gain/element number, peak sidelobe level, and number of reconfigurable modes used, are listed. Compared with the designed array in [10], the proposed array has wider 3-dB beamwidth coverage. Compared with the array in [12], the proposed array has wider peak-gain scanning range and 3-dB beamwidth coverage and a higher peak gain. Furthermore, the proposed array possesses a lower peak

TABLE III

COMPARISON OF THE WIDE-ANGLE SCANNING PERFORMANCE BETWEEN THIS ANTENNA AND [10] AND [12]

	This work	Ref. [10]	Ref. [12]
Scanning range	-75° ~ +75°	-75° to +75°	-60° ~ +60°
3-dB beam width coverage	-90° ~ +90°	-85° to +85°	-68° ~ +68°
Peak scanning gain / Number of elements	15.5 dBi / 8	16.3 dBi / 12	13.2 dBi / 8
Peak scanning gain fluctuation	±0.75 dB	±1.5 dB	±1.9 dB
Peak sidelobe level (SLL)	-7.8 dB	-4.7 dB	-3.5 dB
Reconfigurable modes used	2	3	3

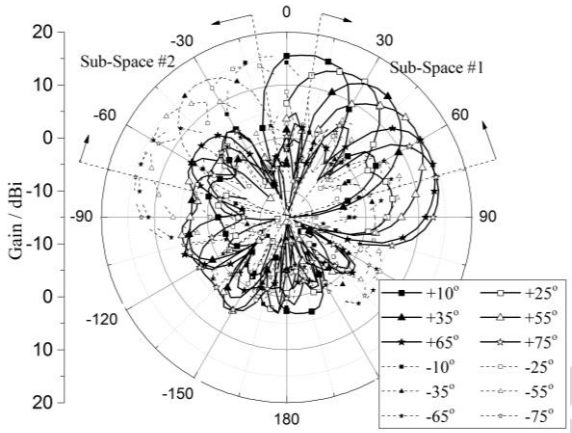

Fig. 11. Measured scanning pattern of the 2×4 element phased array in the *xz* plane.

SLL, small scanning gain fluctuation and less reconfigurable modes used.

IV. CONCLUSION

In this communication, a phased array design with wide-angle scanning capabilities was introduced. Magnetic current sources and a pattern reconfigurable technique were used to design the radiating element. The developed 2×4 array can scan the entire upper half *xoz* plane within its 3 dB beamwidth, while the array achieves a 150° elevation plane scanning with very little gain fluctuation (less than ±0.75 dB). Excellent wide-angle scanning from broadside to endfire is achieved with the proposed system, which can provide an effective design method for wide-angle scanning arrays.

REFERENCES

[1] R. Wang, B.-Z. Wang, X. Ding, and X.-S. Yang, "Planar phased array with wide-angle scanning performance based on image theory," *IEEE Trans. Antennas Propag.*, vol. 63, no. 9, pp. 3908–3917, Sep. 2015.

[2] R. C. Hansen, *Phased Array Antennas*, 2nd ed. New York, NY, USA: Wiley, 2009.

[3] R. J. Mailloux, *Phased Array Antenna Handbook*, 2nd ed. Beijing, China: Publishing House of Electronics Industry, 2008.

[4] C. Gu *et al.*, "Compact smart antenna with electronic beam-switching and reconfigurable polarizations," *IEEE Trans. Antennas Propag.*, vol. 63, no. 12, pp. 5325–5333, Dec. 2015.

[5] Y. X. Cai and Z. W. Du, "A novel pattern reconfigurable antenna array for diversity systems," *IEEE Antennas Wireless Propag. Lett.*, vol. 8, pp. 1227–1230, Nov. 2009.

[6] X. Ding and B.-Z. Wang, "A novel wideband antenna with reconfigurable broadside and endfire patterns," *IEEE Antennas Wireless Propag. Lett.*, vol. 12, pp. 995–998, Aug. 2013.

[7] A. G. Toshev, "Multipanel concept for wide-angle scanning of phased array antennas," *IEEE Trans. Antennas Propag.*, vol. 56, no. 10, pp. 3330–3333, Oct. 2008.

[8] S. E. Valavan, D. Tran, A. G. Yarovoy, and A. G. Roederer, "Planar dual-band wide-scan phased array in X-band," *IEEE Trans. Antennas Propag.*, vol. 62, no. 10, pp. 5370–5375, Oct. 2014.

[9] F. Yang, A. Aminian, and Y. Rahmat-Samii, "A novel surface-wave antenna design using a thin periodically loaded ground plane," *Microw. Opt. Technol. Lett.*, vol. 47, no. 3, pp. 240–245, Nov. 2005.

[10] X. Ding, B.-Z. Wang, and G.-Q. He, "Research on a millimeter-wave phased array with wide-angle scanning performance," *IEEE Trans. Antennas Propag.*, vol. 61, no. 10, pp. 5319–5324, Oct. 2013.

[11] A. Pal, A. Mehta, R. Lewis, and N. Clow, "A wide-band wide-angle scanning phased array with pattern reconfigurable square loop antennas," in *Proc. 9th Eur. Conf. Antenna Propag. (EuCAP)*, Apr. 2015, pp. 1–4.

[12] Y. Y. Bai, S. Q. Xiao, M. C. Tang, Z. F. Ding, and B.-Z. Wang, "Wide-angle scanning phased array with pattern reconfigurable elements," *IEEE Trans. Antennas Propag.*, vol. 59, no. 11, pp. 4071–4076, Nov. 2011.

[13] Y. Hao and C. G. Paini, "Isolation enhancement of anisotropic UC-PBG microstrip diplexer patch antenna," *IEEE Antennas Wireless Propag. Lett.*, vol. 1, no. 1, pp. 135–137, Jan. 2002.

[14] C. A. Balanis, *Antenna Theory, Analysis and Design*, 2nd ed. New York, NY, USA: Wiley, 1997.

[15] J. D. Kraus and R. J. Marhefka, *Antennas: For All Applications*, 3rd ed. New York, NY, USA: McGraw-Hill, 2003.

[16] D. Liu, "Boxed-in slot antenna with space-saving configuration," U.S. Patent 6 483 466 B2, Nov. 19, 2002.

[17] S. Zhang, G. H. Huff, J. Feng, and J. T. Bernhard, "A pattern reconfigurable microstrip parasitic array," *IEEE Trans. Antennas Propag.*, vol. 52, no. 10, pp. 2773–2776, Oct. 2004.

[18] *MA4AGBLP912 Datasheet*. [Online]. Available: http://www.macom.com

[19] D. Peroulis, K. Sarabandi, and L. P. B. Katehi, "Design of reconfigurable slot antennas," *IEEE Trans. Antennas Propag.*, vol. 53, no. 2, pp. 645–654, Feb. 2005.

[20] A. A. Gheethan and D. E. Anagnostou, "Broadband and dual-band coplanar folded-slot antennas (CFSAs) [antenna designer's notebook]," *IEEE Antennas Propag. Mag.*, vol. 53, no. 1, pp. 80–89, Feb. 2011.

AQ:2

AUTHOR QUERIES

AUTHOR PLEASE ANSWER ALL QUERIES

PLEASE NOTE: We cannot accept new source files as corrections for your paper. If possible, please annotate the PDF proof we have sent you with your corrections and upload it via the Author Gateway. Alternatively, you may send us your corrections in list format. You may also upload revised graphics via the Author Gateway.

AQ:1 = Please confirm whether the edits made in the financial section are OK.
AQ:2 = Please confirm the title and also provide the accessed date for ref. [18].

A Wide-Angle Scanning Planar Phased Array with Pattern Reconfigurable Magnetic Current Element

Xiao Ding, You-Feng Cheng, Wei Shao, Hua Li,
Bing-Zhong Wang, and Dimitris E. Anagnostou

***Abstract*— A wide-angle scanning planar phased array with magnetic current elements is proposed. A pattern reconfigurable technique is used to design the element that enhances scanning gain and decreases the sidelobe level throughout the entire scanning range. The array is comprised of eight elements in a 2×4 arrangement with uniform spacing. The proposed phased array operates at 5.8 GHz and can scan with 3 dB beamwidth the entire upper ground elevation plane from -90° to $+90^\circ$ enabled by a two-step pattern reconfigurability mechanism consisting of: 1) coarse-angle scanning and 2) fine-angle scanning. Significant outcomes also include the reduced sidelobe level (less than 7.8 dB) and the particularly small fluctuation (± 0.75 dB) of the gain during scanning over a scanning range of 150° (from -75° to $+75^\circ$ in the elevation plane). With the absence of any structure above the ground level, the high efficiency, and the coverage of the entire upper half-space, this proposed antenna array is very attractive for a variety of phased array applications, particularly those that require a flush-mounted structure.**

***Index Terms*— Antenna arrays, pattern reconfigurable antennas, planar phased arrays, wide-angle beam scanning.**

I. Introduction

Planar phased arrays often require a large ground plane. Specifically, the large ground plane can be considered as an electric or magnetic wall [1]. The analysis conducted in [2] and [3] showed that an electric wall phased array can only scan its main beam direction from -50° to 50° with a gain fluctuation of 4–5 dB, because the beamwidths of the elements in an electric wall phased array are limited, and mutual coupling between elements is strong when the beam is scanned at low elevation (near endfire) angles [4]–[6]. Many related efforts have been carried out to break the bottleneck of the limitation scanning angles. It include a multipanel approach method [7], a wide-beam element method [8], a metasurface technique [9], pattern reconfiguration technique [10]–[12], a mutual coupling reduction method [13], and others.

Among these methods, pattern reconfigurable techniques have been popular and have seen a wide range of applications. For example, a pattern reconfigurable array can collect energy from several switchable directions, and can enhance channel capacity in massive-MIMO communication systems by using pattern diversity.

In this communication, the main challenge and novelty consist of the development and use of flush-mounted slot antenna elements and pattern reconfigurable techniques for the design and creation of a phased array with outstanding wide-angle scanning performance. Specifically, the antenna elements can reconfigure narrow beams to jointly cover the entire top half-space, and thus enable wide-angle scanning. Compared to prior art, it will be shown how slot elements with electric wall modeling are used to reconfigure the pattern and how the scanning performance will be improved (meaning lower sidelobe level, small fluctuation of the gain during scanning, high efficiency, and entire plane of the upper half-space beam coverage). This communication complements well prior research on fundamental wide-angle scanning arrays.

In addition, pattern reconfigurable techniques used in wide-angle scanning arrays have been described. In [10], a millimeter-wave pattern reconfigurable 1×4 linear wide angle scanning phased subarray with reconfigurable feeding networks was design. By dividing the scanning space into multiple regions, a Yagi microstrip antenna using reconfigurable radiating elements comprised a nonuniform linear phased array that could scan up to a maximum of approximately $\pm 60^\circ$ with low sidelobe level [12]. In this communication, the proposed phased array can scan with 3 dB beamwidth that covers an entire plane of the upper elevation plane from -90° to $+90^\circ$, representing a scan covering area improvement of 33% over microstrip elements. First, a novel pattern reconfigurable magnetic current element and its principle of operation are introduced. Then, a 2×4 wide-angle scanning carrier-based planar phased array is proposed and developed. Finally, the wide-angle scanning performance of the proposed phased array is analyzed.

II. Pattern Reconfigurable Magnetic Current Element

A. Element Design

The simplest model of a magnetic current radiator is an aperture antenna, which has an equivalent magnetic current distribution inside the slot parallel to the ground plane. In this situation, the sum of the maximum electric field generated by the magnetic current source and its image source will occur in the endfire direction [14], and the electric field can potentially cover that direction of radiation. This arrangement benefits by achieving wide-angle scanning performance.

The proposed reconfigurable element is based on the boxed-in slot antenna [15], which is cavity-backed and then converted to a Yagi slot [16] by using additional slots as directors or reflector. The structure of the proposed element can be seen as the complementary structure of the printed Yagi antenna [17]. The cavity helps maintain a unidirectional pattern. By altering the length of the slots using p-i-n diodes, the electromagnetic wave can be guided or reflected to or from a specific direction. The geometry of this basic reconfigurable element is shown in Fig. 1.

The basic element comprises five apertures that are carved on a metal ground $L_0 \times W_0$. The center slot $L_S \times W_S$ is excited by using the tip of a coaxial cable that is soldered off-center at the feeding positon L_f for impedance matching purposes, as shown in Fig. 1(b). The additional four slots are parasitic. Their dimensions are $L_1 \times W_1$, and they act as the aforementioned director or reflector depending on how they are configured. In this way, the top layer of the Yagi slot antenna is formed.

Next, a hollow metallic box cavity $L_b \times W_b$ with height $H_b = \lambda/4$ is placed just underneath the excitation slot as shown in Fig. 2(c) and (d) to form the necessary unidirectional pattern and enhance directivity. Under the metal ground, a microstrip substrate ($H_0 = 1$ mm, $\varepsilon_r = 2.2$) is placed and on the backside of the substrate four metallic strips are printed between the above-mentioned slots. In this way, the bottom layer of the Yagi slot antenna is formed.

Third, eight p-i-n diode switches (S_1 through S_8) [18] are grouped in pairs and are embedded in the eight gaps on the strip layer,

Manuscript received June 9, 2016; revised November 4, 2016; accepted November 25, 2016. This work was supported in part by the National Natural Science Foundation of China under Grant #61331007, Grant #61361166008, and Grant #61401065, in part by the U.S. National Science Foundation under Grant #1310400, and in part by the National Aeronautics and Space Administration, EPSCoR, under Grant #NNX15AM83A.

X. Ding, Y.-F. Cheng, W. Shao, H. Li, and B.-Z. Wang are with the Institute of Applied Physics, University of Electronic Science and Technology of China, Chengdu 610054, China (e-mail: xding@uestc.edu.cn; juvencheng1377@gmail.com; weishao@uestc.edu.cn; lihua2006@uestc.edu.cn; bzwang@uestc.edu.cn).

D. E. Anagnostou is with Heriot-Watt University, Edinburgh EH14 4AS, U.K., and also with the South Dakota School of Mines and Technology, Rapid City, SD 57701 USA (e-mail: danagn@ieee.org).

Color versions of one or more of the figures in this communication are available online at http://ieeexplore.ieee.org.

Digital Object Identifier 10.1109/TAP.2016.2637863

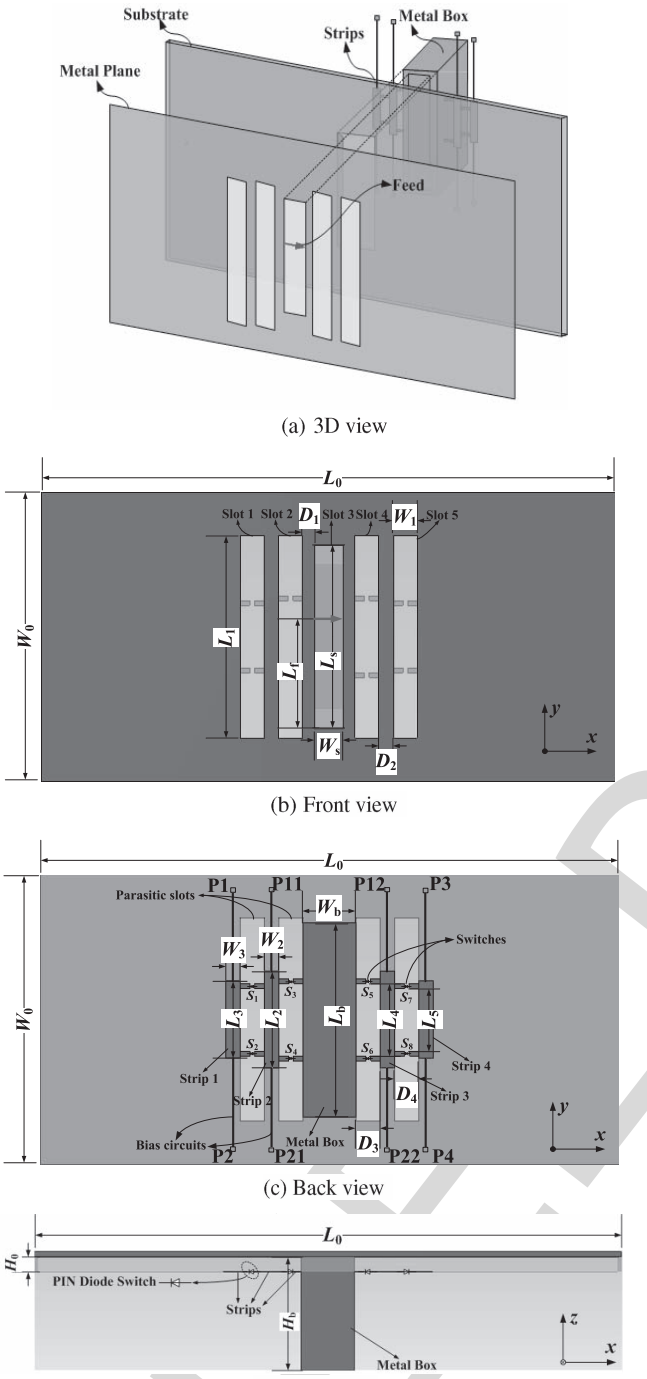

Fig. 1. Structure of the proposed pattern reconfigurable element. (a) 3-D view, (b) front view, (c) detailed back view including the p-i-n diodes, dc bias-circuits, and dc/grounded connection nodes, and (d) side view, showing the structure, the diode placement, and polarity.

as shown in Fig. 1(c). The diodes allow adjusting the electrical length of the parasitic slots by applying a dc biasing voltage, without needing a bandwidth-limiting biasing network [19], [20]. In this way, the slots can act as directors or reflectors on-demand, allowing steering the beam in specific directions. To bias the diodes, a dc voltage is applied to the p-i-n diodes through metal pads at points P12 to P22, while nodes P1–P4 are connected to the ground.

Finally, The operating frequency is determined by the dimensions of the excitation slot and is set here at 5.8 GHz. Adjustment of the size and position of the coplanar parasitic slots and of the noncoplanar strips is necessary as they relate to the excitation slot according to the operating principle of the Yagi antenna.

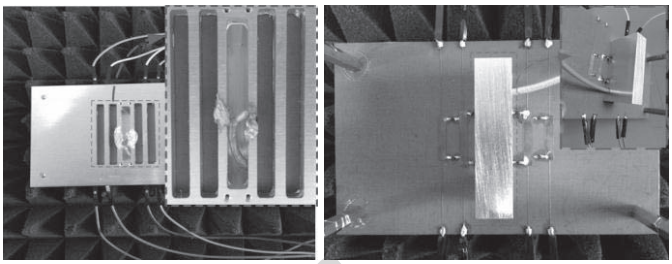

Fig. 2. Photographs of the reconfigurable element. (a) Top view including feeding position and white plastic adhesive. (b) Back view including coaxial feeding cable, hollow metallic box with a hole in the side, dc bias-circuits, and p-i-n diodes.

TABLE I
PHYSICAL ANTENNA DIMENSIONS

Parameter	Value (mm)	Parameter	Value (mm)	Parameter	Value (mm)
L_0	120	L_2, L_4	20	W_1	5
L_S	38	L_3, L_5	16	W_2, W_3	3
L_b	40	W_0	70	D_1	2.5
L_f	32.5	W_S	6	D_2	3
L_1	42	W_b	11	D_3, D_4	5

Fig. 2 shows the photo of the proposed reconfigurable element, and the inset images show details of the expanded connection part of the center. It is noteworthy that a small hole is opened on one side of the hollow metallic box, for the feeding coaxial cable to pass through and reach the top of the slot. The outer conductor of the cable is soldered to one side of the slot, and plastic adhesive is used to fix the bonding pad. The inner conductor of the cable is soldered to the other side of the slot and is also fixed with plastic adhesive. The physical parameters of the structure are summarized in Table I.

B. Reconfiguration Principle

The proposed basic antenna element can reconfigure its radiation pattern in three different directions, or modes. These are two tilted modes with higher directivity, and one broadside radiation mode at x-axis.

First, the first mode is enabled when P12 (or P22) is connected to the $V_{\text{bias}} = 3$ V, and P3 (or P4) is connected to ground [Fig. 1(c)]. When the diode switches S_5 through S_8 are ON, the strips at the right side connect together and the current distribution on that side is altered in a way that makes the RF current to pass through the p-i-n diodes and feed the right sided slots. This causes the electrical length of the right slots to become shorter than the left ones. The (smaller) right slots guide the electromagnetic radiation while the (larger) left slots reflect it. This steers the radiation pattern to the right. A detailed 3-D current distribution in this case is shown in Fig. 3.

Based on geometric structure and intuition, the effective length has been used to explain the reconfigurable patterns as above. A more detailed explanation is provided below. When all the diode switches in the left slot are OFF and more capacitance and inductance are introduced, then the resonant frequency of the parasitic slot decreases to be lower than that of the driven slot. When the antenna operates near the resonant frequency of the driven slot, the parasitic slot is inductive and acts as a reflector. At the same time, all the diode

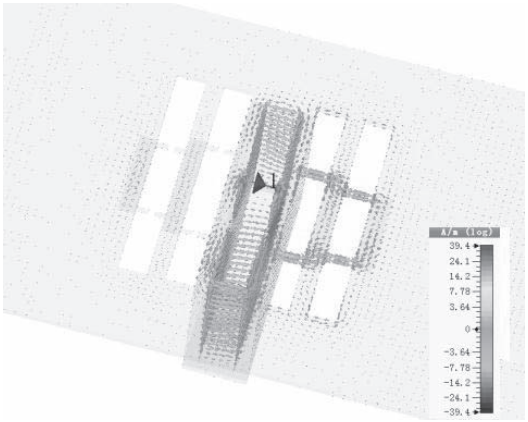

Fig. 3. 3-D current distribution of the reconfigurable element when the p-i-n diodes on the right side are activated, making the slots narrower. The right side slots direct the electromagnetic wave, while the larger slots on the left side reflect it.

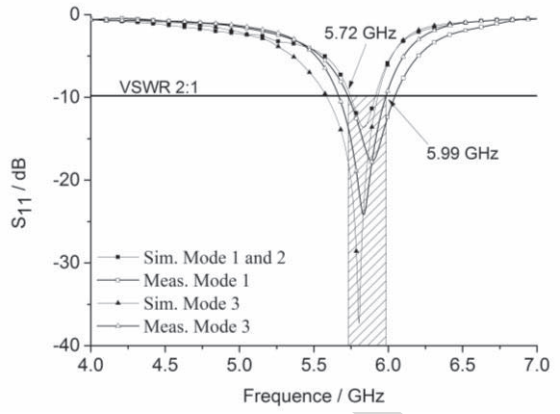

Fig. 4. Measured and simulated reflection coefficient of the antenna illustrating the similar bandwidth and matching for all configurations. Modes 1 and 2 are symmetric so only one is shown.

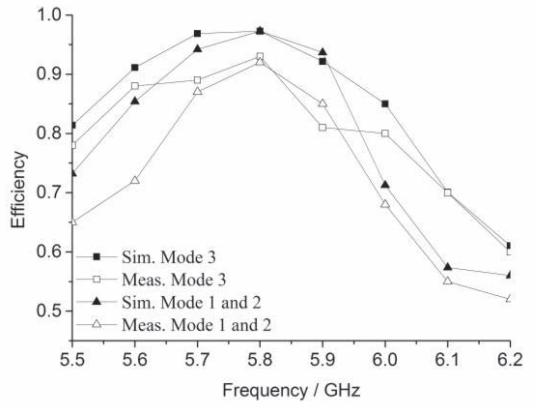

Fig. 5. Measured and simulated efficiencies of the antenna are very high (above 90%) at the resonant frequency.

switches in the right slot are ON, then the resonant frequency of the parasitic slot increases to be higher than that of the driven slot, the parasitic slot is capacitive and acts as a director at approximately the resonant frequency of the driven element.

Second, the second tilted mode can be obtained in the reverse way, by connecting P11 (or P21) to the V_{bias} and P1 (or P2) to the ground. This steers the radiation pattern to the left.

Finally, the third mode is obtained when all the diodes are OFF. Then, the excited slots radiates omnidirectionally like a traditional single slot antenna, at right angles to the largest dimension of the slot, while the box structure ensures a broadside direction with small front-to-back ratio.

Moreover, the control mechanism for the p-i-n diodes can be explained as follows. When P11 and P21 are connected to the power supply with $V_{\text{bias}} = 3$ V, S_1–S_4 are ON. When P12 and P22 are connected to the power supply with $V_{\text{bias}} = 3$ V, S_5–S_8 are ON. Since the bias lines are very narrow, the RF impedance is very high and little RF energy can get through it. Furthermore, the bias current has minimal impact on the antenna performance since the bias circuits are located below the ground plane and separated by the radiation slot.

C. Results and Analysis

The measured reflection coefficient at each mode is shown in Fig. 4. All modes have approximately the same bandwidth (5.7–6 GHz), as expected since the radiating element does not alter from configuration to configuration. The simulated and measured efficiencies of the antenna are very high as expected by the radiating element that is a metallic slot (Fig. 5).

Fig. 6 shows the radiating performance of the proposed antenna. The cross polarization patterns at each reconfigurable mode are below −20 dB. Also, due to the symmetry of the proposed structure, the radiation performance of Modes 1 and 2 [Fig. 6(a) and (b)] is almost symmetric. Moreover, the measured gain of Modes 1 and 2 is higher than 7 dBi. The pattern of Mode 3 [Fig. 6(c)] is indeed broadside about 5 dBi gain. The higher directivity of the tilted beam modes is conducive to the wide-angle scanning while the antenna maintains a high scanning gain level at large scanning angles.

The effect of varying the strips length [see Fig. 1(c)] on the copolarization and cross-polarization patterns of the proposed element was studied through Mode 2 as an example. Fig. 7 (below) was added to show the effect of the strips with varying length on the copolarization and cross-polarization patterns.

In Fig. 7, as the length of the strips increasing, the directivity of the element decreases gradually, the maximum radiation will point toward a lower elevation angle at −65° with increasing SLLs. On the other hand, decreasing the strips length steers the direction of maximum radiation to point toward a higher elevation angle at −55°, which means the element will not be able to cover the low elevation areas within its 3 dB beamwidth. In other word, compared to the 3 dB beamwidth obtained by the selected values, this joint 3 dB beamwidth become narrower. This narrow beamwidth is not good for wide-angle scanning.

In addition, a similar study was carried out to help understand how the length of the strips affects matching. Fig. 8 shows the S_{11} variation tendency when the length of the strips is varied. Increasing the length lowers the resonant frequency of the antenna. Decreasing the length increases the operation frequency while it degrades the matching. Since the strips are not on the driven element itself [Fig. 1(c)], they affect the driven element only through mutual coupling. Antenna matching is not affected as fields are not reflected back to the driven element to alter the excitation currents. This was accomplished through accurate selection of lengths of the D/R slots in a similar way to Yagi antennas.

III. Wide-Angle Scanning Phased Array and Its Scanning Performance

The aforementioned pattern reconfigurable antenna was next used to develop a 2×4 uniform wide-angle scanning planar phased array.

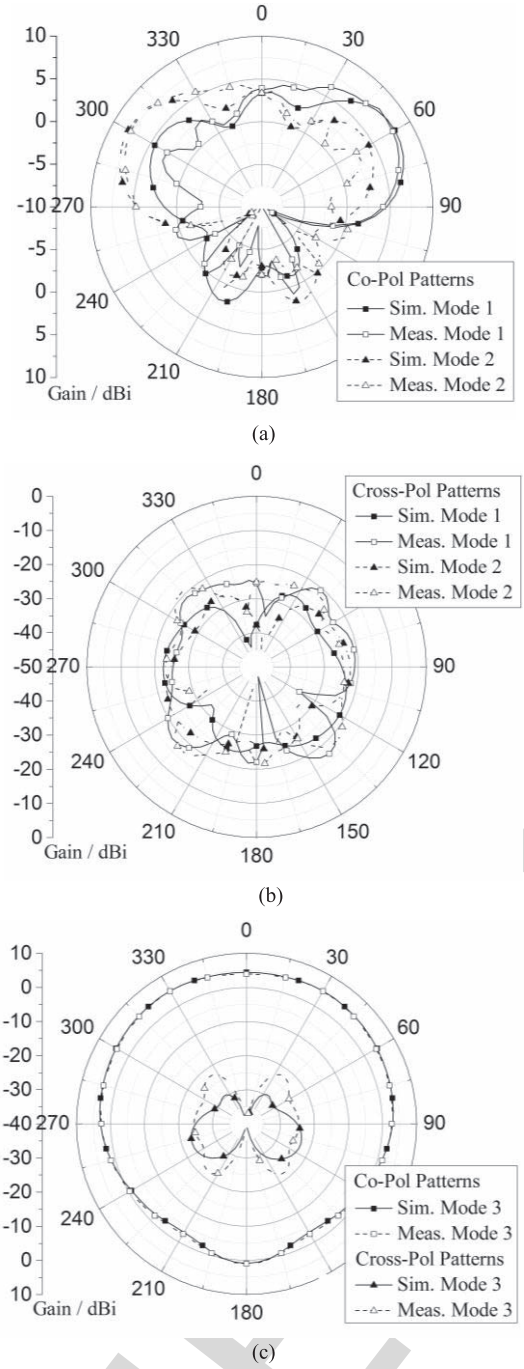

Fig. 6. Measured and simulated radiation patterns. (a) Copolarization of Mode 1 when the beam is steered to the right and Mode 2 when the beam is steered to the left. (b) Cross-polarization of Modes 1 and 2. (c) Third mode when the beam is not steered (broadside mode with flat gain). The measurements validate the simulations.

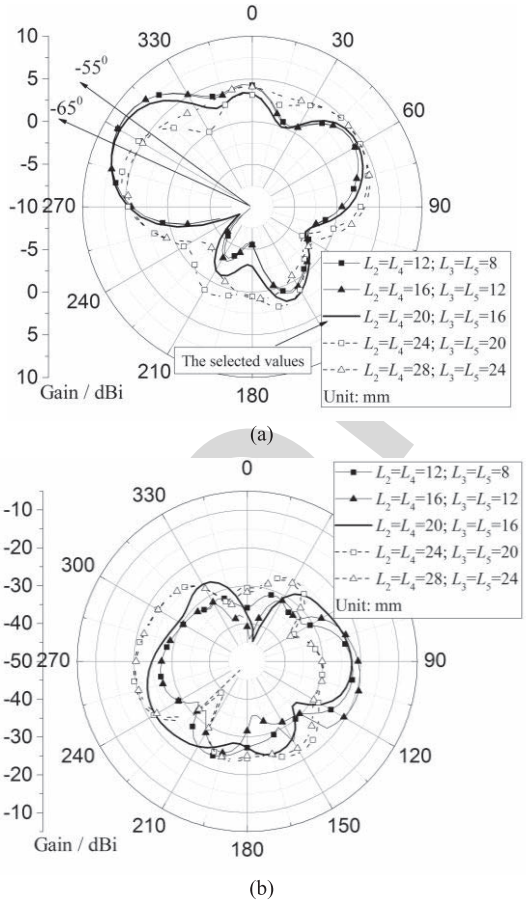

Fig. 7. Simulated radiation patterns at the second reconfigurable mode with variable strips length. (a) Copolarization patterns including the variation gain, direction of the maximum radiation, SLLs, and 3 dB beamwidth. (b) Cross-polarization always below −20 dB patterns.

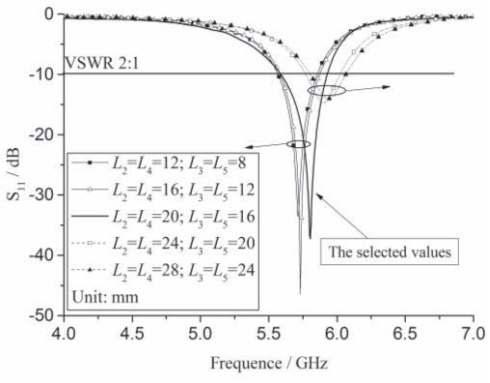

Fig. 8. Simulated S_{11} trends over variable strips length. Increasing the length lowers the resonant frequency of the antenna. Decreasing the length increases the operation frequency while it degrades the matching.

Next, a wide-angle scanning method with pattern reconfigurable techniques is presented first, and the scanning performance is analyzed.

A. Wide-Angle Scanning Array

A uniform wide-angle scanning carrier-based planar phased planar array was developed by combining eight of the proposed antennas in a 2×4 arrangement, and is shown in Fig. 9. The numbers ①, ②, … ⑧ represent each antenna's feeding port. It is worth noting that the structure of some elements on the array differs slightly from the proposed antenna. In order to reduce the spacing between adjacent elements, the two outer slots of the middle elements have been removed and the edge elements maintained their outer slots.

The distance between each element in the x-direction is set to $d_{\text{array}} = 0.54\lambda$, where λ is the free-space wavelength at 5.8 GHz and 0.6λ in y-direction. The total size of the phased array is 198 mm × 114 mm.

The designed 2×4 array was fabricated and is shown in Fig. 10, along with the measurement system that had to be developed and

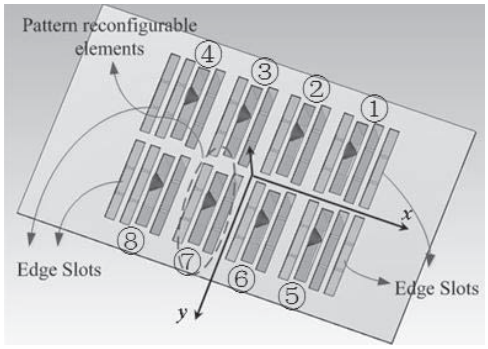

Fig. 9. Geometry of the wide-angle scanning phased array in a 2 × 4 arrangement.

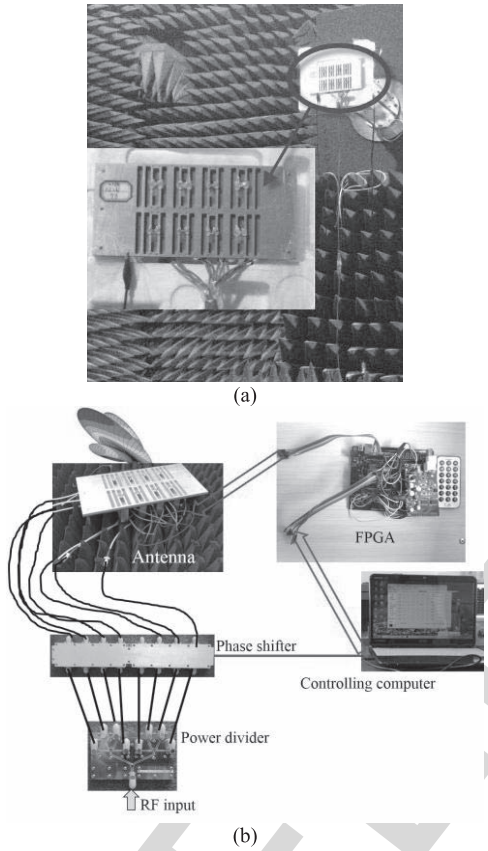

Fig. 10. (a) Photograph of the eight-element phased array measured in the anechoic chamber. (b) Photographs of the measurement system setup of the array.

which contains 6-b digital phase shifters, a 1:8 power divider, phase-compensated low-loss coaxial cables, an field-programmable gate array (FPGA) control device, and a control computer. In this setup, an FPGA provides a dc voltage to turn the p-i-n diodes ON or OFF, and control the operating reconfigurable modes. A 1:8 equal power divider is used to divide the input signal into eighths (i.e., the output signals at the output ports of the divider has equal amplitude and phase). Then the eight signals are supplied to eight phase shifters, where different phase differences are provided to the adjacent elements of the proposed array. During this process, the proposed phased array begins scanning.

The technique to realize wide-angle scanning in conjunction with pattern reconfigurability of the array is divided in two steps.

TABLE II
PERFORMANCE OF THE 2 × 4 PHASED ARRAY WITH PATTERN RECONFIGURABLE ELEMENTS

	Scanning performance values				3 dB joint cover range
	θ_{max}	Gain (dBi)	MSLL (dB)	Θ_{BW} 3dB	
Mode 1 (right steering)	+10°	15.5	-11.8	26°	-7° to +90°
	+25°	14.7	-9.3	32°	
	+35°	14.6	-10.8	31°	
	+55°	14	-8.5	37°	
	+65°	14.5	-8	38°	
	+75°	14.2	-7.8	37°	
	θ_{max}	Gain (dBi)	MSLL (dB)	Θ_{BW} 3dB	
Mode 2 (left steering)	-10°	15.5	-11.8	26°	-90° to +7°
	-25°	14.7	-9.4	32°	
	-35°	14.5	-10.8	31°	
	-55°	14.2	-8.6	36°	
	-65°	14.5	-8	38°	
	-75°	14.2	-7.7	36°	

1) *Coarse-Angle Scanning:* The scanning space of the array is divided into several subspaces and each subspace, respectively, matches with one of the reconfigurable narrow beams (modes) of the elements.
2) *Fine-Angle Scanning:* When all the reconfigurable elements have been set to a reconfigurable mode, beam scanning in the corresponding subspace can be fine-tuned by adjusting the phase shift of each element, as in traditional phased arrays.

B. Wide-Angle Scanning Performance

As mentioned earlier, the scanning space of this array is divided into two subspaces. Modes 1 and 2 are used to match these subspaces. When all elements are set to Mode 1, their scanning subspace (subspace 1) is from +10° to +75° in the *xoz* plane and the phase shifts between elements are provided by the 6-b phase shifters. In addition, when all elements are set to Mode 2, the scanning results can be obtained in subspace 2 (i.e., in the *xoz* plane from −75° to −10°).

The scanning performance was tested at 5.8 GHz with linear progressive phase shift from element to element. The array can scan subspaces 1 and 2 by pointing the main-lobe from $\theta = -75°$ to $+75°$ with extremely small fluctuation (±0.75°) of the gain during scanning over a scanning range of 150° (from −75° to +75°), while the 3 dB scanning beamwidth can cover a large range from −90° to +90° in the elevation plane. These are also shown by the scanning patterns in Fig. 11. The maximum scanning gain is 15.5 dBi and the minimum is 14 dBi, indicating less than 1.5 dB scanning gain fluctuation. This scanning performance is excellent for many applications in modern communication systems. The scanning gain, maximum peak sidelobe level (MSLL), scanning 3 dB beamwidth (BW), and the subspace range values are all listed in Table II.

A comparison between the proposed phased array and those in [10] and [12] are shown in Table III. The wide-angle scanning performance, including the peak-gain scanning range, 3-dB beamwidth coverage, peak gain/element number, peak sidelobe level, and number of reconfigurable modes used, are listed. Compared with the designed array in [10], the proposed array has wider 3-dB beamwidth coverage. Compared with the array in [12], the proposed array has wider peak-gain scanning range and 3-dB beamwidth coverage and a higher peak gain. Furthermore, the proposed array possesses a lower peak

TABLE III

COMPARISON OF THE WIDE-ANGLE SCANNING PERFORMANCE BETWEEN THIS ANTENNA AND [10] AND [12]

	This work	Ref. [10]	Ref. [12]
Scanning range	-75° ~ +75°	-75° to +75°	-60° ~ +60°
3-dB beam width coverage	-90° ~ +90°	-85° to +85°	-68° ~ +68°
Peak scanning gain / Number of elements	15.5 dBi / 8	16.3 dBi / 12	13.2 dBi / 8
Peak scanning gain fluctuation	±0.75 dB	±1.5 dB	±1.9 dB
Peak sidelobe level (SLL)	-7.8 dB	-4.7 dB	-3.5 dB
Reconfigurable modes used	2	3	3

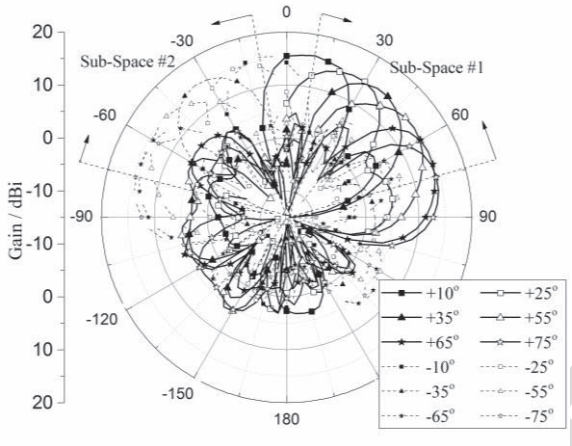

Fig. 11. Measured scanning pattern of the 2×4 element phased array in the *xz* plane.

SLL, small scanning gain fluctuation and less reconfigurable modes used.

IV. CONCLUSION

In this communication, a phased array design with wide-angle scanning capabilities was introduced. Magnetic current sources and a pattern reconfigurable technique were used to design the radiating element. The developed 2×4 array can scan the entire upper half *xoz* plane within its 3 dB beamwidth, while the array achieves a 150° elevation plane scanning with very little gain fluctuation (less than ±0.75 dB). Excellent wide-angle scanning from broadside to endfire is achieved with the proposed system, which can provide an effective design method for wide-angle scanning arrays.

REFERENCES

[1] R. Wang, B.-Z. Wang, X. Ding, and X.-S. Yang, "Planar phased array with wide-angle scanning performance based on image theory," *IEEE Trans. Antennas Propag.*, vol. 63, no. 9, pp. 3908–3917, Sep. 2015.

[2] R. C. Hansen, *Phased Array Antennas*, 2nd ed. New York, NY, USA: Wiley, 2009.

[3] R. J. Mailloux, *Phased Array Antenna Handbook*, 2nd ed. Beijing, China: Publishing House of Electronics Industry, 2008.

[4] C. Gu *et al.*, "Compact smart antenna with electronic beam-switching and reconfigurable polarizations," *IEEE Trans. Antennas Propag.*, vol. 63, no. 12, pp. 5325–5333, Dec. 2015.

[5] Y. X. Cai and Z. W. Du, "A novel pattern reconfigurable antenna array for diversity systems," *IEEE Antennas Wireless Propag. Lett.*, vol. 8, pp. 1227–1230, Nov. 2009.

[6] X. Ding and B.-Z. Wang, "A novel wideband antenna with reconfigurable broadside and endfire patterns," *IEEE Antennas Wireless Propag. Lett.*, vol. 12, pp. 995–998, Aug. 2013.

[7] A. G. Toshev, "Multipanel concept for wide-angle scanning of phased array antennas," *IEEE Trans. Antennas Propag.*, vol. 56, no. 10, pp. 3330–3333, Oct. 2008.

[8] S. E. Valavan, D. Tran, A. G. Yarovoy, and A. G. Roederer, "Planar dual-band wide-scan phased array in X-band," *IEEE Trans. Antennas Propag.*, vol. 62, no. 10, pp. 5370–5375, Oct. 2014.

[9] F. Yang, A. Aminian, and Y. Rahmat-Samii, "A novel surface-wave antenna design using a thin periodically loaded ground plane," *Microw. Opt. Technol. Lett.*, vol. 47, no. 3, pp. 240–245, Nov. 2005.

[10] X. Ding, B.-Z. Wang, and G.-Q. He, "Research on a millimeter-wave phased array with wide-angle scanning performance," *IEEE Trans. Antennas Propag.*, vol. 61, no. 10, pp. 5319–5324, Oct. 2013.

[11] A. Pal, A. Mehta, R. Lewis, and N. Clow, "A wide-band wide-angle scanning phased array with pattern reconfigurable square loop antennas," in *Proc. 9th Eur. Conf. Antenna Propag. (EuCAP)*, Apr. 2015, pp. 1–4.

[12] Y. Y. Bai, S. Q. Xiao, M. C. Tang, Z. F. Ding, and B.-Z. Wang, "Wide-angle scanning phased array with pattern reconfigurable elements," *IEEE Trans. Antennas Propag.*, vol. 59, no. 11, pp. 4071–4076, Nov. 2011.

[13] Y. Hao and C. G. Paini, "Isolation enhancement of anisotropic UC-PBG microstrip diplexer patch antenna," *IEEE Antennas Wireless Propag. Lett.*, vol. 1, no. 1, pp. 135–137, Jan. 2002.

[14] C. A. Balanis, *Antenna Theory, Analysis and Design*, 2nd ed. New York, NY, USA: Wiley, 1997.

[15] J. D. Kraus and R. J. Marhefka, *Antennas: For All Applications*, 3rd ed. New York, NY, USA: McGraw-Hill, 2003.

[16] D. Liu, "Boxed-in slot antenna with space-saving configuration," U.S. Patent 6 483 466 B2, Nov. 19, 2002.

[17] S. Zhang, G. H. Huff, J. Feng, and J. T. Bernhard, "A pattern reconfigurable microstrip parasitic array," *IEEE Trans. Antennas Propag.*, vol. 52, no. 10, pp. 2773–2776, Oct. 2004.

[18] *MA4AGBLP912 Datasheet*. [Online]. Available: http://www.macom.com

[19] D. Peroulis, K. Sarabandi, and L. P. B. Katehi, "Design of reconfigurable slot antennas," *IEEE Trans. Antennas Propag.*, vol. 53, no. 2, pp. 645–654, Feb. 2005.

[20] A. A. Gheethan and D. E. Anagnostou, "Broadband and dual-band coplanar folded-slot antennas (CFSAs) [antenna designer's notebook]," *IEEE Antennas Propag. Mag.*, vol. 53, no. 1, pp. 80–89, Feb. 2011.

AQ:2

AUTHOR QUERIES

AUTHOR PLEASE ANSWER ALL QUERIES

PLEASE NOTE: We cannot accept new source files as corrections for your paper. If possible, please annotate the PDF proof we have sent you with your corrections and upload it via the Author Gateway. Alternatively, you may send us your corrections in list format. You may also upload revised graphics via the Author Gateway.

AQ:1 = Please confirm whether the edits made in the financial section are OK.
AQ:2 = Please confirm the title and also provide the accessed date for ref. [18].